Magnetic-field induced gap and staggered susceptibility in the $S = 1/2$ chain $[PM{\cdot}Cu(NO_3)_2{\cdot}(H_2O)_2]_n$ (PM = pyrimidine)

2000 J. Phys.: Condens. Matter 12 8495

(http://iopscience.iop.org/0953-8984/12/39/312)

J. Phys.: Condens. Matter **12** (2000) 8495–8509. Printed in the UK PII: S0953-8984(00)14157-8

Magnetic-field induced gap and staggered susceptibility in the $S = 1/2$ chain $[PM{\cdot}Cu(NO_3)_2{\cdot}(H_2O)_2]_n$ (PM = pyrimidine)

R Feyerherm†§, S Abens†, D Günther†, T Ishida‡, M Meißner†, M Meschke†, T Nogami‡ and M Steiner†

† Hahn-Meitner-Institute (HMI), 14109 Berlin, Germany
‡ Department of Applied Physics and Chemistry, The University of Electro-Communications, Chofu, Tokyo 182-8585, Japan

E-mail: feyerherm@hmi.de

Received 23 May 2000

Abstract. Single-crystal magnetic susceptibility and specific heat studies of the one-dimensional copper complex $[PM{\cdot}Cu(NO_3)_2{\cdot}(H_2O)_2]_n$ (PM = pyrimidine) show that it behaves like a uniform $S = 1/2$ antiferromagnetic Heisenberg chain, characterized by the exchange parameter $J/k_B = 36$ K. Specific heat measurements in the applied magnetic field, however, reveal the formation of a field-induced spin excitation gap, whose magnitude depends on the magnitude and direction of the field. This behaviour is inconsistent with the ideal $S = 1/2$ Heisenberg chain. In the low-temperature region, a contribution to the susceptibility, approximately proportional to $1/T$, is observed which varies strongly with the varying direction of the magnetic field. The field-induced gap and the $1/T$ contribution are largest for the same field direction. Previous observations of a field-induced gap in the related compounds copper benzoate and Yb_4As_3 have been explained by the alternating g tensor and alternating Dzyaloshinkii–Moriya interaction, producing an effective staggered magnetic field at the Cu and Yb ions. We apply this model to $[PM{\cdot}Cu(NO_3)_2{\cdot}(H_2O)_2]_n$ and obtain a consistent quantitative explanation of the low-temperature susceptibility, the field-induced gap and their dependence on the magnetic-field direction.

1. Introduction

Chain compounds of magnetic ions with low spin have attracted the interest of chemists and physicists for more than three decades because they exhibit pronounced quantum effects. Well known examples are the gapless continuum of spin excitations in the uniform $S = 1/2$ antiferromagnetic Heisenberg chain [1] and the appearance of the Haldane gap in the integer spin antiferromagnetic chain [2].

The theory of the ideal uniform $S = 1/2$ antiferromagnetic Heisenberg chain in the magnetic field is well established and usually describes the observed properties in real systems very well. Recently, the theoretical prediction of magnetic-field dependent incommensurate low-energy modes could be verified for the first time by inelastic neutron scattering on copper benzoate [3, 4]. In this compound however, specific heat measurements revealed the opening of a spin excitation gap in the magnetic field [4]. A similar behaviour was found in Yb_4As_3 [5]. This behaviour is not consistent with the uniform Heisenberg chain model. It was shown theoretically [6–8] that it arises from the staggered local g tensor of neighbouring Cu or

§ Full address of corresponding author: Dr Ralf Feyerherm, Hahn-Meitner-Institut, Glienicker Strasse 100, 14109 Berlin, Germany.

0953-8984/00/398495+15$30.00

Yb ions and the alternating Dzyaloshinkii–Moriya (DM) interaction, leading—in an applied uniform field—to an effective staggered magnetic field perpendicular to the uniform field. The corresponding Hamiltonian can be mapped onto the sine–Gordon model. Exact results for the field and temperature dependence of the gap can be derived. The staggered magnetic field was predicted to cause a divergent contribution to the low-temperature magnetic susceptibility [6]. Although such a staggered susceptibility appears to be present in previously reported data on one-dimensional $S = 1/2$ antiferromagnets (e.g., in copper benzoate [9]), it was usually not recognized as intrinsic to the chains but associated with chain defects or paramagnetic impurities.

In this work we present single-crystal electron spin resonance (ESR), magnetic susceptibility and specific heat studies of the one-dimensional copper pyrimidine complex $[PM \cdot Cu(NO_3)_2 \cdot (H_2O)_2]_n$ recently synthesized [10]. We show that this compound behaves like an almost ideal uniform $S = 1/2$ antiferromagnetic Heisenberg chain characterized by the single exchange parameter $J/k_B = 36$ K. The system exhibits an alternating Cu g tensor similar to copper benzoate.

In the low-temperature region a contribution to the susceptibility approximately proportional to $1/T$ is observed which varies strongly with varying direction of the magnetic field. Specific heat measurements in the applied magnetic field reveal the formation of a field-induced spin excitation gap whose size depends on the magnitude and direction of the field. We demonstrate that the field-induced gap and the $1/T$ contribution are largest for the same field direction.

We apply the theoretical model described above to our data on $[PM \cdot Cu(NO_3)_2 \cdot (H_2O)_2]_n$ and give a quantitative explanation of the low-temperature susceptibility, the field-induced gap, and their dependence on the magnitude and direction of the magnetic field. We are able to disentangle the contributions from the alternating g tensor and the DM interaction and to determine the DM interaction vector. Our study constitutes the first systematic study of the orientation dependence of the staggered susceptibility and provides clear experimental evidence for the direct relation between the field-induced gap and the staggered susceptibility predicted by theory.

The structure of this paper is as follows. After describing the experimental procedures in the next section we briefly summarize important points concerning the crystal structure in section 3. Then we present and discuss the experimental results of the ESR (section 4) and susceptibility measurements (section 5). In section 5 we also present the determination of the DM interaction from the susceptibility results. In section 6 we present and discuss the specific heat data. The article ends with a final discussion (section 7) and the conclusions (section 8).

2. Experimental

Single crystals of the title compound have been grown by slow evaporation of the equimolar aqueous solution of copper nitrate and pyrimidine [10]. The crystals show well defined facets and the principal axes can be identified easily. Powder samples have been obtained by grinding small single crystals. Unit cell parameters at various temperatures were determined from high-resolution X-ray powder diffraction data collected with a HUBER–Guinier diffractometer 645 using Cu-K_α radiation. Neutron powder diffraction was carried out on a partly deuterated sample, $[PM \cdot Cu(NO_3)_2 \cdot (D_2O)_2]_n$, at 2 K and at room temperature using the fine resolution powder diffractometer E9 at HMI and a standard Orange cryostat. The neutron wavelength was 1.7964 Å. All powder diffraction data were refined with the Rietveld method using the FULLPROF package [11].

ESR measurements were carried out on a small crystal of about 5 mg mass at 9.5 GHz

with a Bruker ESP300E spectrometer.

Susceptibility and magnetization measurements were carried out using an MPMS Squid magnetometer (Quantum Design). A single crystal of about 50 mg mass was prepared for mounting on the MPMS horizontal rotator which allowed for rotating the sample around an axis vertical to the magnetic field. Measurements were carried out at temperatures between 1.8 and 300 K in varying magnetic fields H up to 50 kOe and for a number of different orientations. At all temperatures, the susceptibility $\chi = M/H$ was constant in a field range up to about 10 kOe. The χ data were corrected for diamagnetic and sample holder contributions that were determined experimentally by extrapolation of the high-temperature susceptibility data for $1/T \to 0$. The corrections were small and consistent with calculated estimates. Susceptibility values are given per mole Cu. An additional susceptibility measurement at a field of 90 kOe was carried out on a smaller sample (used also for the heat capacity measurements) using a home made Squid magnetometer [12].

Heat capacity was measured using an Oxford Instrument 9 T MagLab calorimeter with ^{3}He refrigerator. Flat crystal plates of approx. $0.5 \times 3 \times 3$ mm^3 (8 mg mass) were prepared, with the plate normal parallel or perpendicular to the b-axis. The crystals were attached to the sapphire chip, which is the central part of the calorimeter, using a small amount of a grease containing alumina powder (Wakefield 120–2). The normal on the chip surface is perpendicular to the magnetic field, so that the orientation of a crystal relative to the magnetic field could be varied by rotating the crystal in the plane of the chip. The estimated accuracy of alignment is about $\pm 5^\circ$. The temperature dependence of the specific heat was measured for different magnetic field values and varying field directions.

3. Crystal structure

A detailed account of the structure is given in [13]. Here we summarize the facts that are important for the interpretation of the experimental data presented below. $[PM \cdot Cu(NO_3)_2 \cdot (H_2O)_2]_n$, (full chemical name: catena-diaquadinitrato[μ-pyrimidine-N^1:N^3]-copper(II)), crystallizes in a monoclinic structure, space group $C2/c$ with four formula units per unit cell. The lattice constants from single-crystal x-ray diffraction are $a = 12.404$ Å, $b = 11.511$ Å, $c = 7.518$ Å, $\beta = 115.0^\circ$ [13]. Powder x-ray diffraction results in $a = 12.3760$ Å, $b = 11.4972$ Å, $c = 7.5051$ Å, $\beta = 114.97^\circ$ at 297 K and $a = 12.1405$ Å, $b = 11.4376$ Å, $c = 7.4557$ Å, $\beta = 113.82^\circ$ at 10 K. These values are in close agreement with the neutron powder diffraction data on the partly deuterated sample. Rietveld refinements of the powder diffraction data show that the low-temperature crystal structure is essentially the same as at room temperature.

Figure 1 shows the structure of a single chain. All Cu ions are crystallographically equivalent and located at centres of inversion symmetry. They form uniformly spaced chains running parallel to the short ac diagonal ($d_{Cu-Cu} = 5.71$ Å at 10 K). The Cu ions are linked by the N–C–N moieties of pyrimidine, which constitute the intrachain magnetic exchange pathway. The interchain Cu–Cu distance is 6.84 Å.

The Cu coordination is a distorted octahedron, built from an almost square N–O–N–O equatorial plane and two O in the axial positions. In this approximately tetragonal local symmetry, the local principal axis of each octahedron is tilted from the ac plane by $\pm 29.4^\circ$. As this axis almost coincides with the g tensor principal axis (see section 4), for a pair of Cu nearest neighbours the g tensors are staggered. For a general magnetic field direction these ions become magnetically inequivalent. This structural feature of $[PM \cdot Cu(NO_3)_2 \cdot (H_2O)_2]_n$ is very similar to the behaviour of Cu benzoate and constitutes the prerequisite for the appearance of the staggered field and therefore for the magnetic field-induced gap and the staggered susceptibility.

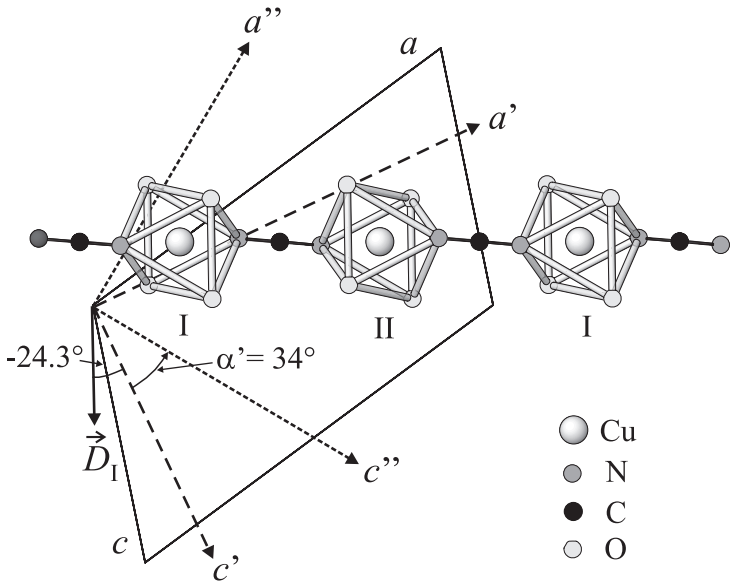

Figure 1. A single chain of $[PM \cdot Cu(NO_3)_2 \cdot (H_2O)_2]_n$ viewed along the *b*-axis. For clarity, only the ions forming elongated, distorted octahedra around the central Cu ions and the N–C–N bridges are shown. The local principal axis of each octahedron is tilted from the *ac* plane (the paper plane) by $\pm 29.4^\circ$ (+/− for Cu I/II), Consequently, the octahedra are staggered, leading to an alternating Cu *g* tensor. The definition of the axes a', c', a'' and c'' used in the text is also shown. For the orientation of the DM interaction vector, $\vec{D}$, see section 5.

In the following we will use a coordinate system related to the *g* tensor principal axes. We define the projection of the local tetragonal axis onto the *ac* plane as c' and the normal on c' in the *ac* plane as a' (see figure 1). The axes c' and a' are at angles of 14° and 104°, respectively, with respect to the *c*-axis. We define the angle α' as the angle with respect to the c' direction. In this notation, the chain direction is at $\alpha' = 64^\circ$. We introduce the direction of the maximum (minimum) staggered susceptibility and field-induced gap in sections 5 and 6 as c'' (a'').

4. ESR

Figure 2 shows the angular dependence of the *g* factor measured by ESR at room temperature [14]. We find $g_{a'} = 2.073(2)$, $g_b = 2.152(2)$, $g_{c'} = 2.290(2)$. Within the experimental uncertainty these values are in good agreement with susceptibility data, see section 5. The observed *g* factor results from an averaging of the individual *g* tensors of the two magnetically inequivalent Cu ions. Assuming tetragonal local symmetry, the principal values of the local *g* tensor are $g_\parallel = 2.362$ and $g_\perp = 2.073$. The associated angular dependence of the *g* factor of the individual ions is shown in figure 2 as dotted lines. The tilt angle of the *g* tensor principal axes from the *ac* plane determined from the ESR data is $\pm 30.8^\circ$, where the sign alternates along the chain. Therefore, for a pair of Cu neighbours the *g* tensors are staggered with a relative angle of 61.6°. The *g* value anisotropy is consistent with the usual behaviour of Cu^{2+} ions in an elongated octahedral environment, assuming that the unpaired electron occupies a $d_{(x^2-y^2)}$ orbital.

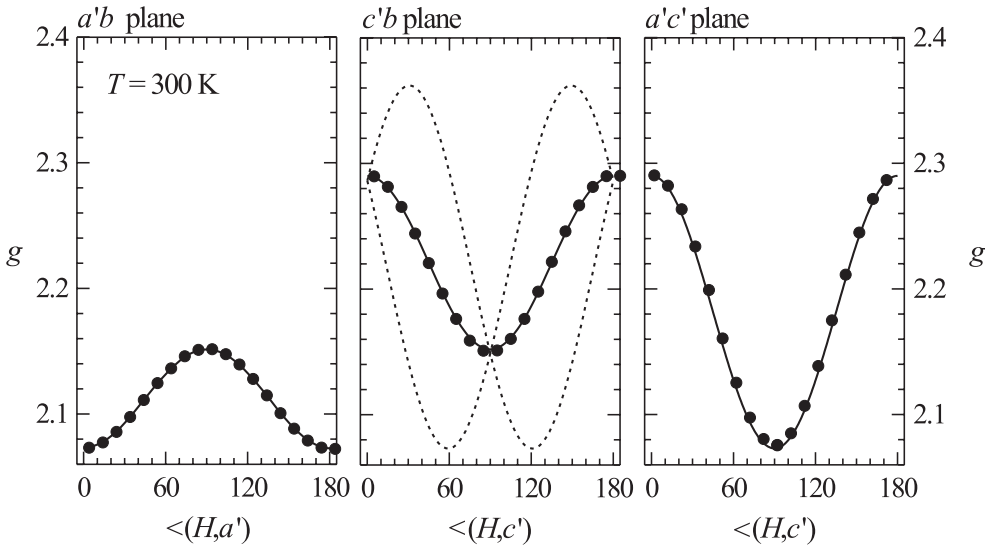

Figure 2. Orientation dependence of the Cu g factor (circles) in $[PM \cdot Cu(NO_3)_2 \cdot (H_2O)_2]_n$ determined by room-T ESR. The observed g factor in the $c'b$ plane results from an averaging of the individual g tensors (dotted line) of the magnetically inequivalent Cu ions.

In the coordinate frame $a'bc'$ the g tensor $\overleftrightarrow{g}$ assumes the form

$$\overleftrightarrow{g} = \begin{pmatrix} 2.073 & 0 & 0 \\ 0 & 2.149 & \pm 0.127 \\ 0 & \pm 0.127 & 2.287 \end{pmatrix} = \begin{pmatrix} g_{xx} & 0 & 0 \\ 0 & g_{yy} & \pm g_s \\ 0 & \pm g_s & g_{zz} \end{pmatrix} = \overleftrightarrow{g}_u \pm \overleftrightarrow{g}_s \,. \quad (1)$$

The effective g value for an arbitrary field direction is given by $g = |\overleftrightarrow{g}\,\vec{H}|/|\vec{H}|$. The off-diagonal elements of $\overleftrightarrow{g}$ are staggered (+/− for Cu I/II in figure 1). Accordingly, the terms $\overleftrightarrow{g}_u$ and $\overleftrightarrow{g}_s$ denote the uniform and the staggered parts of the g tensor. We can interpret $\vec{h} = \overleftrightarrow{g}_s\,\vec{H}$ as staggered magnetic field. It is perpendicular to the applied field for $H \parallel b$ or in the ac plane, corresponding to the experimental geometries used in this paper. The contribution to the total staggered field from the DM interaction will be discussed in section 5.

The ESR signal has Lorentzian shape as expected for an exchange-coupled system. The observed linewidth of $\Delta H \approx 20$ Oe is small compared to other antiferromagnetic Heisenberg chain compounds (e.g. $\Delta H \approx 200$ Oe for Cu-benzoate) and apparently shows no indication of line broadening due to spin diffusion. A small orientation dependence (±8 Oe) of the linewidth is observed which is governed by the anisotropic exchange interaction containing contributions from the J anisotropy and the DM interaction. The dipole–dipole interaction is supposed to be negligible due to the large Cu–Cu distance. Since the detailed temperature and orientation dependence of the linewidth from the DM interaction appears to be still a matter of controversy [15, 16], we refrain from a detailed analysis of the linewidth before temperature dependent data are available.

5. Susceptibility

A preliminary report of the single-crystal susceptibility data has been already given in [17]. It was shown that the temperature dependence of the susceptibility, $\chi(T)$, exhibits the general

features of the $S = 1/2$ antiferromagnetic chain, namely a characteristic maximum and non-zero susceptibility as $T \to 0$. Using the theoretical temperature dependence of the susceptibility of the uniform $S = 1/2$ antiferromagnetic Heisenberg chain calculated first by Bonner and Fisher [18], the exchange parameter $J/k_B = 36$ K was determined (note that in [17] $2J$ was used instead of J). In addition, the principal values of the g tensor, $g_{a'} = 2.05(2)$, $g_b = 2.11(2)$, $g_{c'} = 2.27(2)$ were obtained, which agree well with the ESR data. The value of the exchange parameter J was found to be isotropic within the experimental uncertainty ($\pm 2\%$). It is expected [7] that the effect of a small J anisotropy to the behaviour described in the following is much smaller than the effect of the staggered g tensor and the DM interaction and therefore it is neglected.

In [17], an upturn of $\chi(T)$ below 10 K was reported that could be described by an additional contribution proportional $1/T$. It exhibited a strong dependence on the magnetic field direction and therefore was interpreted as intrinsic property of the Cu chains and associated with the staggered susceptibility predicted to arise from the staggered field.

We provide an improved analysis of the low-temperature susceptibility data and new experimental results as function of the magnetic field. We apply the theory for the effect of the alternating g tensor and the alternating DM interaction to our data and obtain a quantitative explanation of the experimental results.

The temperature dependence of the magnetic susceptibility of the uniform $S = 1/2$ antiferromagnetic Heisenberg chain was calculated recently in detail by Eggert *et al* [19] using the Bethe ansatz. This result differs significantly from the Bonner–Fisher result for $T < 0.25J/k_B$. The result of Eggert *et al* can be written as

$$\chi(T) = g^2\left(\frac{N_A\mu_B^2}{4k_B}\right)F\left(\frac{J}{k_BT}\right)\frac{1}{T} = \frac{C_u}{T}F\left(\frac{J}{k_BT}\right) \tag{2}$$

where $F(x = J/k_BT)$ is an empirical rational function. We find

$$F(x) = \frac{1 + 0.085\,16x + 0.233\,51x^2}{1 + 0.733\,82x + 0.136\,96x^2 + 0.535\,68x^3} \tag{3}$$

for $T > 0.05J/k_B$. Note that $F(x) \to 1$ for $T \to \infty$. The theoretical result of Eggert *et al* is displayed in figure 3 together with equation (2) and the Bonner–Fisher result. For $T > 0.5J/k_B$ all three curves coincide.

Figure 4 shows the experimental $\chi(T)$ data for $[PM{\cdot}Cu(NO_3)_2{\cdot}(H_2O)_2]_n$ for two different magnetic field orientations in the ac plane. The observed temperature dependence of χ can be well described by

$$\chi(T) = \chi_u(T) + C_s/T \tag{4}$$

where χ_u is the uniform susceptibility of the chain, given by equation (2). We identify $\chi_s = C_s/T$ with the staggered susceptibility predicted to arise from the staggered field. Therefore, we neglect a logarithmic correction for $T \ll J/k_B$ [7] that varies slowly below 10 K. This is necessary because no analytical formula for the T dependence of the staggered susceptibility is available which is valid in the full T range of the experiment.

The staggered susceptibility for both orientations determined from equation (4) is shown in figure 4(a) as dashed lines. While it is very pronounced for one direction, it vanishes almost completely for the other. Figure 5 shows the angular dependence of the coefficient C_s of the staggered susceptibility in the ac plane, derived from the $\chi(T)$ data for these and for several other field orientations. The maximum is observed at an angle $\alpha' = 34^\circ$ with respect to the c' axis, defining the axis c''. In the minimum, the staggered susceptibility appears to vanish. The direction c' is determined from the same data set as c'', namely by the maximum g value

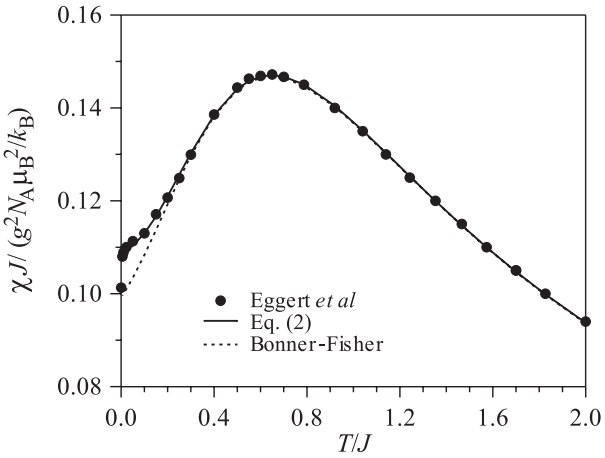

Figure 3. Temperature dependence of the normalized susceptibility for the uniform $S = 1/2$ antiferromagnetic Heisenberg chain, calculated by Eggert *et al* [19] (●), equation (2) (——), and the Bonner–Fisher result [18] (– – –). The latter curve differs significantly from the exact result by Eggert *et al* for $T < 0.25J/k_B$. In contrast, equation (2) describes the exact results very well for $T > 0.05J/k_B$.

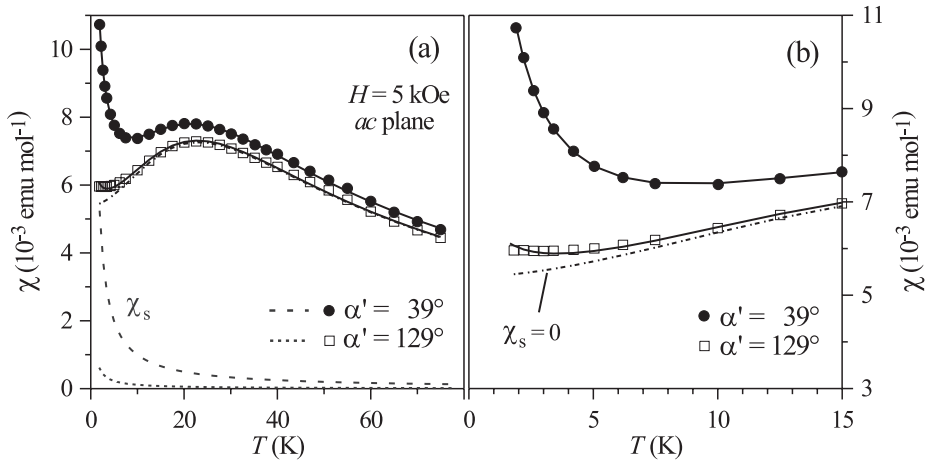

Figure 4. (*a*) Temperature dependence of χ for two orientations in the ac plane together with fits of equation (4). The staggered susceptibility determined from equation (4) for both orientations is drawn as dashed lines. For $\alpha' = 129^\circ$ the behaviour assuming $\chi_S = 0$ is marked as dashed–dotted line. (*b*) A blow up of the low-temperature region.

in the ac plane. Therefore, the experimental error on the angle $\alpha' = 34^\circ$ between these two axes is small ($\pm 2^\circ$).

We wish to point out that for $\alpha' = 129^\circ$, close to the minimum staggered susceptibility, the $\chi(T)$ data appear not to show any indication of a steep upturn at low T, as described by the term C_s/T but rather an asymptotically constant value as $T \to 0$ (see figure 4(b)). Therefore, we believe that the residual value of C_s in the minimum is an artefact resulting from an inaccurate description of the actual case of *zero* staggered field by equation (2). Further arguments which support this view arise from the specific heat data discussed in the following section. Since

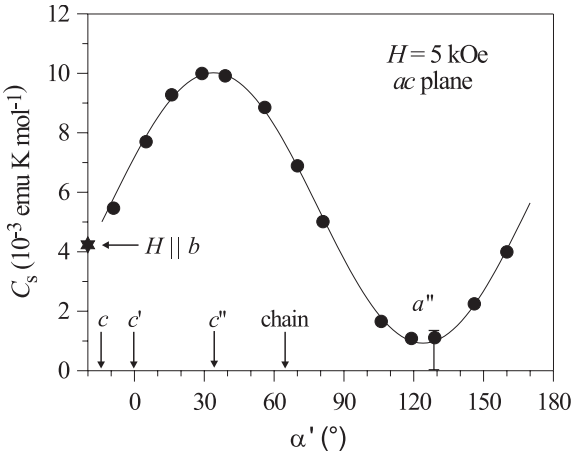

Figure 5. Angular dependence of C_s in the ac plane. The solid curve is a fit to a $\cos^2$ angular dependence. The maximum is located at $\alpha' = 34^\circ$, defining the axis c''. The error bar refers to a possible systematic error (see text). The C_s value for $H \parallel b$ is marked by an arrow. (Note that in a related figure in [17], the relative angle between the axes c and c' is erroneously marked as 9°. In the experiment, the nominal c axis was aligned visually before the measurements with the MPMS horizontal rotator. We associate the 5° offset of c' from its nominal position in [17] to a small original misalignment of the c-axis and the slip of the horizontal rotator.)

there is a relation between the staggered susceptibility and the field-induced gap, an upper limit for the residual value of C_s can be estimated from the residual gap for $H \parallel a''$ (section 6). We obtain a value of $1.3 \times 10^{-3} C_{s,\max}$, which is negligible. This gives a possible systematic error for the values for C_s close to the minimum staggered field that is marked in figure 5, as an error bar. It is unclear how strongly the C_s values for the other orientations are affected, but the corresponding systematic error is presumably smaller.

The deviation of the measured χ for $\alpha' = 129^\circ$ from the theoretical behaviour described by equation (2) may be associated with contributions from chain defects to the susceptibility, which do not necessarily have to follow a $1/T$ temperature dependence.

The field dependence of the staggered susceptibility has been studied for $\alpha' = 39^\circ$, i.e., an orientation with large $1/T$ contribution, by measurement of $\chi(T)$ in different magnetic fields. Figure 6 shows the results for magnetic fields of 0.05, 5, 50 and 90 kOe. No significant variation of the $\chi(T)$ curves is observed between 0.05 and 5 kOe. Field-dependent magnetization measurements (not shown) reveal that the staggered susceptibility becomes smaller for applied field values larger than 10 kOe. At 50 kOe the reduction is about 25%, at 90 kOe it is almost 50%. We associate this effect with the saturation of the staggered magnetization.

In the following we interpret our susceptibility data on the basis of the theoretical model derived in [6, 7]. The Hamiltonian of the Heisenberg chain in a magnetic field can be written as

$$\boldsymbol{H} = \sum_j [J\vec{S}_j \cdot \vec{S}_{j+1} - \mu_B(\overleftrightarrow{g}\ \vec{H}) \cdot \vec{S}_j - (-1)^j \vec{D} \cdot (\vec{S}_j \times \vec{S}_{j+1})] \tag{5}$$

where we use a general form of the Zeeman term and include the DM interaction, which is characterized by the vector $\vec{D}$. The orientation of $\vec{D}$ is partly restricted by the lattice symmetry. Since neighbouring Cu ions are symmetry related by a rotation about the two-fold axis parallel to b, $\vec{D}$ must lie in the ac plane and alternate along the chain (+/− for Cu I/II in figure 1). This is accounted for by the term $(-1)^j$.

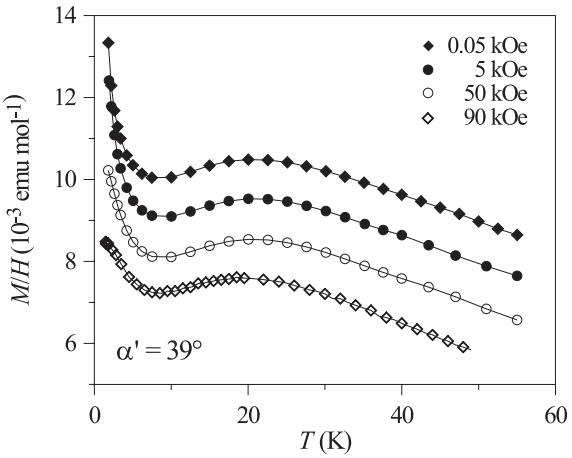

Figure 6. Temperature dependence of the susceptibility for an orientation with large staggered susceptibility for different magnetic field values. For clarity, the three upper curves are shifted upwards by 10^{-3}, 2×10^{-3} and 3×10^{-3} emu mol^{-1}. No significant difference is observed between 0.05 kOe and 5 kOe. At 50 kOe the $1/T$ contribution is reduced by about 25%, at 90 kOe by about 50%. The solid lines are guides to the eye.

Due to the alternating DM interaction and the canting of the g tensor, the uniform external field $\vec{H}$ induces a staggered field $\vec{h}$. The contribution from the staggered g tensor has been already discussed in section 4 (equation (1)). The contribution from the DM interaction follows from a transformation in which it is eliminated by a rotation in spin space around $\vec{D}$ by an angle $\pm \arctan(D/J)/2$ on even/odd sites. Defining the field direction as the z-axis and taking into account that $\vec{h}$ is approximately perpendicular to $\vec{H}$ and $h \ll H$, the Hamiltonian finally can be rewritten as

$$\boldsymbol{H} = \sum_j [J\vec{S}_j \cdot \vec{S}_{j+1} - \mu_B g^z H S_j^z - \mu_B (-1)^j h S_j^x] \tag{6}$$

which corresponds to a Heisenberg model with orthogonal uniform and staggered fields. A small exchange anisotropy is neglected. Here, g^z is the effective g value for the specific magnetic field orientation, $g^z = |\overleftrightarrow{g}_u \vec{H}|/|\vec{H}|$, and h is the absolute value of the total staggered field $\vec{h}$,

$$\vec{h} \approx \frac{1}{2J}\vec{D} \times \overleftrightarrow{g}_u \vec{H} + \overleftrightarrow{g}_s \vec{H}. \tag{7}$$

The first term is the contribution from the DM interaction. It is largest for $\vec{H}$ perpendicular to $\vec{D}$. The second term results from the staggered g tensor. For a general magnetic-field direction the two contributions in equation (5) need not be parallel, but for all cases of interest they are here.

For $T \ll J/k_B$ the staggered magnetic field leads to a contribution to the measured susceptibility which scales with the ratio $c = h/H$ [7]:

$$\chi_s(T) = 0.2779c^2 \left(\frac{N_A \mu_B^2}{k_B}\right) \frac{\ln^{1/2}(J/k_B T)}{T}. \tag{8}$$

Since the logarithmic term varies slowly with T, at low T the staggered susceptibility varies approximately like C/T. Using this equation, the ratio c can be determined directly from the C_s data determined above (figure 5). The logarithmic correction leads to a correction

factor of $\ln^{-1/4}(J/k_BT)$ for the values of c. For 1.8 K, the minimum temperature of the present experiment, it gives a factor of 0.76 as the maximum logarithmic correction (for higher T the factor is closer to unity). This results in the corrected values $c_{c''} = 0.235$ and $c_b = 0.152$. An alternative fit procedure, replacing C_s/T in equation (4) by equation (8) and setting the logarithmic correction equal to unity for $T > J/k_B$, results in essentially equal values, $c_{c''} = 0.238$ and $c_b = 0.156$. We observe, however, that the overall T dependence of the staggered susceptibility is described better by the pure C_s/T term in equation (4). According to the theory the staggered field should vanish in the minimum, and thus we set $c_{a''}$ zero.

From these experimental values for c the value of g_s and the two unknown components of $\vec{D}$ are determined as follows. We write the magnetic field in the ac plane $\vec{H} = H(\sin\alpha', 0, \cos\alpha')$, the field along the b-axis $\vec{H} = H(0, 1, 0)$, and the DM vector $\vec{D} = D(\sin\alpha, 0, \cos\alpha)$. Inserting these definitions and the experimental values into equation (7) results in three equations for the three variables g_s, D, α:

$$c_{c''} = \frac{D}{2J}(g_{xx}\sin\alpha'\cos\alpha - g_{zz}\cos\alpha'\sin\alpha) + g_s\cos\alpha' \tag{9}$$

$$0 = \frac{D}{2J}(g_{xx}\cos\alpha'\cos\alpha + g_{zz}\sin\alpha'\sin\alpha) - g_s\sin\alpha' \tag{10}$$

and

$$c_b^2 = \left(\frac{g_{yy}D}{2J}\right)^2 + g_s^2 + \frac{g_s g_{yy}D}{J}\sin\alpha \tag{11}$$

where $\alpha' = 34^\circ$, and the values for g_{ii} are given by equation (1). We obtain two solutions, namely

$$g_s = 0.129,\ D/J = 0.139,\ \alpha = -24.3^\circ \tag{12}$$

and

$$g_s = 0.059,\ D/J = 0.173,\ \alpha = -43.1^\circ. \tag{13}$$

Notably, the value of α and the ratio g_s/D do not depend on the logarithmic correction used above. The agreement between the value for g_s in equation (12) and the expected one (0.127, see equation (1)) is excellent. We conclude that the first solution is the more likely one. The value for D is in very good agreement with the usual estimate $D/J = \Delta g/\overline{g} = 0.13$ (where $\overline{g}$ is the average g value). Both contributions to the staggered field are of approximately the same magnitude.

Finally, in the frame $a'bc'$ the DM interaction vector assumes the form

$$\vec{D} = 0.139J(-0.4115, 0, 0.9114). \tag{14}$$

The orientation of $\vec{D}$ is approximately perpendicular to the chain direction as shown in figure 1.

6. Specific heat

The temperature dependence of the specific heat in zero magnetic field in the full temperature range 0.4–15 K (in figure 7(a) data are shown up to 4.5 K) can be well described by the sum of the specific heat for the uniform $S = 1/2$ Heisenberg chain, c_{BF}, calculated first by Bonner and Fisher [18], and a term proportional to T^3 from the thermal excitation of lattice vibrations,

$$c(T) = c_{BF} + bT^3. \tag{15}$$

with $b = 0.0015$ J mol^{-1} K^{-3}. Characteristic for c_{BF} is the approximately T-linear behaviour at low temperatures with a slope $C/T(T \to 0) = 0.7R/(J/k_B)$, where R is the gas constant.

In the present experiment, figure 7(a), we find a value of 0.156 J mol^{-1} K^{-2}, which is in very good agreement with the expected value (0.162 J mol^{-1} K^{-2}) for $J/k_B = 36$ K. No indications are found for three-dimensional long-range ordering down to 0.38 K. Therefore, the interchain interactions are smaller than the intrachain interaction by at least a factor of 10^{-2}.

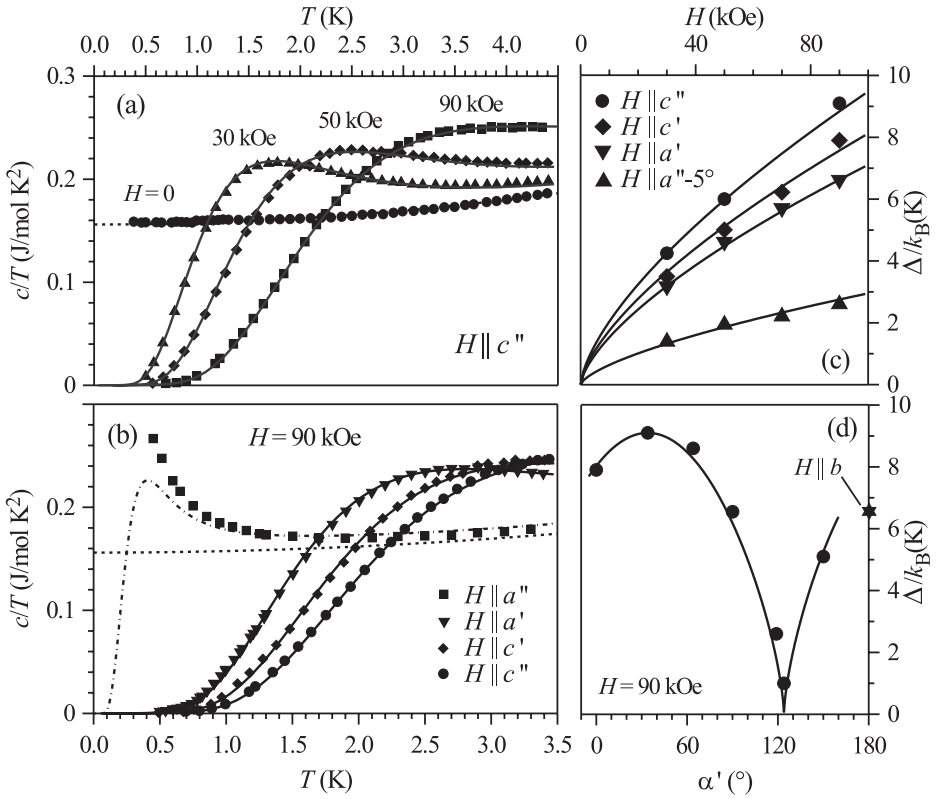

Figure 7. (a) Temperature dependence of the specific heat of $[PM \cdot Cu(NO_3)_2 \cdot (H_2O)_2]_n$ for different values of the applied field and $H \parallel c''$, i.e., the orientation with maximum staggered field; (b) $c/T(T)$ curves for an applied field of 90 kOe and different field orientations. For clarity, not all measured data are shown. The solid curves in (a) and (b) are fits to equation (16). The dashed-dotted curve in (b) is a calculation for $\Delta = 1$ K; (c) the magnetic field dependence of the gap determined from these fits for different field orientations. The solid lines are fits to the equation $\Delta = aH^{2/3}$; (d) the angular dependence of the gap in the ac plane for an applied field of 90 kOe. The solid line is a fit to the expected $\cos^{2/3}$ angular dependence. The maximum is observed at $H \parallel c''$.

The temperature dependence of the specific heat c for the field orientation $H \parallel c''$, corresponding to the maximum staggered field, is shown in figure 7(a) as c/T for various values of the magnetic field H. By application of a magnetic field, the low-temperature behaviour changes from T-linear to exponential, which is characteristic for the formation of a magnetic-field-induced spin excitation gap. At k_BT values larger than the gap, the c/T versus T curves approach the ideal-chain behaviour asymptotically. The entropy is moved from low to higher T and the total entropy is conserved. A similar behaviour has been reported for copper benzoate [4] and Yb_4As_3 [5].

The data can be well described by the equation

$$c(T) = c_{SG} + bT^3. \tag{16}$$

where c_{SG} is the numerical solution for the specific heat for the sine–Gordon model [20]. The fit results are shown in figure 7(a) as solid lines. The model has only two parameters, namely the magnetic-field dependent spin wave velocity v_S and the gap Δ. These parameters determine the absolute magnitude of the specific heat and the position of the inflection point of the low-T 'exponential' part, respectively. The spin wave velocity at zero field is given by $v_S(0) = \pi J/2$.

Apparently, equation (16) describes the observed temperature dependence of the specific heat very well for all field values $H \parallel c''$. The maximum field-induced gap observed in our experiments is $\Delta/k_B = 9.1$ K in a field of 90 kOe. We observe a small reduction of the spin wave velocity by the application of the external field, namely $v_S = 0.968 v_S(0)$ for $H = 50$ kOe and $v_S = 0.937 v_S(0)$ for $H = 90$ kOe. This is consistent with theoretical expectations [18].

Figure 7(b) shows the temperature dependence of the specific heat for $H = 90$ kOe and various field orientations in the ac plane. As expected from the angular dependence of the staggered field derived from the susceptibility, the field-induced gap is also strongly dependent of the field orientation. Again, the solid lines show fits to equation (16) with $v_s = 0.937 v_s(0)$ for all field orientations.

Equation (16) does not describe the data well in the case of a very small field-induced gap as observed for $H \parallel a''$. Here, the gap is so small that the exponentially activated behaviour at $T \ll \Delta/k_B$ can not be observed experimentally. The dashed-dotted curve in figure 7(b) is a calculation, using $v_s = 0.937 v_s(0)$ and $\Delta/k_B = 1$ K. Apparently, the measured specific heat increases more strongly with decreasing T than expected from the sine–Gordon model. The origin of this behaviour is unclear. It may be associated with additional field-induced contributions to the specific heat, perhaps related to anisotropic exchange interactions, that are suppressed for large gap values. However, the value $\Delta/k_B = 1$ K may serve as a rough estimate of the gap in 90 kOe for $H \parallel a''$.

Comparing the observed gap values with the magnitude of the external field, we find that in the present experiments $\Delta \leqslant \mu_B g H$ is fulfilled for all specific heat data. Actually, the interesting case $\Delta \approx \mu_B g H$ is realized for $H \parallel c''$ and small field values (e.g., $\Delta/k_B \approx \mu_B g H/k_B \approx 4$ K in a field of 30 kOe). In this regime, the absolute value of the gap is related to the staggered field by [6, 19]

$$\Delta/J \approx 1.777(\mu_B h/J)^{2/3} \ln^{1/6}(J/\mu_B g H). \tag{17}$$

Since $h = cH$ and the logarithmic term varies only slowly with H, this results in an approximate scaling of the gap with field as $\Delta \propto H^{2/3}$. The magnetic-field dependence of the gap for several field orientations is shown in figure 7(c). It approximately follows the expected power law. For $H \parallel c''$ we find $\Delta = 0.44 H^{2/3}$ if Δ is measured in K and H in kOe.

The angular dependence of the gap in the ac plane for a field of 90 kOe is shown in figure 7(d). Since h varies with the cosine of the field orientation, an approximate $\cos^{2/3}$ behaviour is expected from equation (17). The data follows this angular dependence very well. The maximum is found at $H \parallel c''$, i.e., the same orientation where the maximum staggered susceptibility is observed. According to theory, the gap should vanish in the minimum ($H \parallel a''$). Experimentally, however, a small residual gap is observed. It is important to note, however, that due to the steep angular dependence close to the minimum (see figure 7(d)), already a small misalignment of 2% will lead to a measured gap of about 10% of the maximum value. We therefore associate the observed residual gap to a small alignment error in our specific heat measurements.

Using equation (17) we can determine values for $c = h/H$ from the experimental values for the gap and compare these to the results from the susceptibility measurements (section 5). We observe a scaling $\Delta = 0.44 H^{2/3}$ for $H \parallel c''$ and $\Delta = 0.33 H^{2/3}$ for $H \parallel b$, resulting

in $c_{c''} = 0.282$ and $c_b = 0.184$ if we take the logarithmic correction for an average field of $H = 60$ kOe. These values are about 20% larger than the values $c_{c''} = 0.235$ and $c_b = 0.152$, determined above from the susceptibility data. Given the uncertainty of the magnitude of the logarithmic corrections for the two different experiments we consider the agreement between the c values from the susceptibility data and the specific heat as good. We wish to note that the values for the ratio $c_{c''}/c_b$, which does not depend on the applied logarithmic corrections, agree very well.

We conclude that the specific heat data are consistent with the DM interaction vector determined in section 5.

7. Discussion

The theoretical model developed in [6, 7] relates both the divergent low-T contribution to the susceptibility and the field-induced gap to the staggered magnetic field produced by the staggered g tensor and the alternating DM interaction. Apparently, it gives a consistent description of the temperature and orientation dependence of the magnetic susceptibility and the magnetic field-induced gap observed in $[PM \cdot Cu(NO_3)_2 \cdot (H_2O)_2]_n$. A similar set of parameters describes the field and orientation dependence of the susceptibility and the specific heat very well. Our study therefore constitutes clear experimental evidence for the direct relation between the field-induced gap and the staggered susceptibility predicted by theory.

Similar behaviour as in $[PM \cdot Cu(NO_3)_2 \cdot (H_2O)_2]_n$ has been reported before only in two other compounds, namely copper benzoate [4, 6] and Yb_4As_3 [5, 8].

Copper benzoate has a crystal structure quite similar to that of $[PM \cdot Cu(NO_3)_2 \cdot (H_2O)_2]_n$ and was studied in much detail. The staggered susceptibility, however, has not been discussed to date, although it was apparently already observed in the original publication [9]. There, no explanation was given. Usually, divergent contributions to the susceptibility of Heisenberg chains were not recognized as intrinsic to the chains but were associated with chain defects and paramagnetic impurities. [3] and [7] discuss a peculiar behaviour of the susceptibility for Cu benzoate in very low fields ($H \leqslant 50$ Oe), whose magnitude and field-dependence is in disagreement with the theory. It was suggested that these effects may be associated with interchain interactions rather than with the staggered susceptibility.

We have reinvestigated the susceptibility for Cu benzoate recently [22] and found in moderate applied fields of a few kOe the characteristic field orientation dependent $1/T$ contribution. It is largest for $H \parallel c$ and undetectable for $H \parallel a$, basically confirming the original data of [9]. The staggered susceptibility is of similar magnitude as in $[PM \cdot Cu(NO_3)_2 \cdot (H_2O)_2]_n$, namely $c = 0.20(2)$ for $H \parallel c$. This value is in very good agreement with the value $h/gH = 0.111$ derived from the field-induced gap for an orientation close to the c axis in [7]. The detailed analysis leads to a value of $D/J = 0.13$ and an orientation of $\vec{D}$ almost perpendicular to the chain direction [7], very similar to our observations for $[PM \cdot Cu(NO_3)_2 \cdot (H_2O)_2]_n$.

For the other example of the combined occurrence of the field-induced gap and the staggered susceptibility, Yb_4As_3 [5, 8], specific heat and susceptibility data have been published only for polycrystalline or multidomain samples to date. Therefore the orientation dependence is not known.

Counterexamples are the well-known $S = 1/2$ Heisenberg chains $CuPy_2Cl_2$ (Py =pyridine) [23], frequently abbreviated CPC, and $Cu(C_4H_4N_2)(NO_3)_2$ [24]. In these compounds, the g tensors are not staggered and the symmetry does not allow for a DM interaction. Consequently, no low-temperature $1/T$ contribution can be identified in the susceptibility data. Specific heat measurements on the latter compound show no gap in the

external magnetic field [25].

Given the present results, we speculate that in all Heisenberg chain compounds with similar structural features as copper benzoate or $[PM \cdot Cu(NO_3)_2 \cdot (H_2O)_2]_n$, namely a symmetry that produces a staggered g tensor, a significant low-temperature divergent contribution to the susceptibility and a field-induced gap is to be expected. For a number of $S = 1/2$ compounds in which a contribution from chain defects and paramagnetic impurities to the susceptibility was reported previously, it actually might be intrinsic to the chains and be explained by the effective staggered magnetic field. Therefore, single-crystal studies of such compounds are highly desirable.

8. Conclusion

We have shown that $[PM \cdot Cu(NO_3)_2 \cdot (H_2O)_2]_n$ behaves like an almost ideal one-dimensional uniform $S = 1/2$ antiferromagnetic Heisenberg chain, characterized by the exchange parameter $J/k_B = 36$ K. At temperatures $T \ll J/k_B$, the magnetic susceptibility differs from the ideal Heisenberg chain model. A contribution to the susceptibility approximately proportional $1/T$ is observed. Specific heat measurements in applied magnetic field reveal the formation of a field-induced spin excitation gap. Both the susceptibility and the specific heat depend strongly on the magnitude and direction of the field. We demonstrated that the field-induced gap and the $1/T$ contribution are largest for the same field direction.

We have applied a theory to our experimental data that relates the observed effects to the staggered local g tensor on neighbouring Cu ions and the alternating DM interaction. These lead to an effective staggered magnetic field perpendicular to the applied uniform field. This theoretical model gives a consistent description of the temperature and orientation dependence of the magnetic susceptibility—including the low-temperature divergent contribution—and the magnetic field-induced gap. From the experimental data a consistent value for the DM interaction vector $\vec{D}$ could be determined.

Our study constitutes the first systematic study of the orientation dependence of the staggered susceptibility and provides clear experimental evidence for the direct relation between the field-induced gap and the staggered susceptibility predicted theoretically.

Acknowledgments

We gratefully acknowledge useful discussions concerning the theory with I Affleck, F H L Essler, M Oshikawa, K Penc and H Shiba, as well as experimental support by F Kubanek and D Többens. We thank B Pilawa for performing the ESR measurements.

References

[1] Des Cloizeaux J and Pearson J J 1962 *Phys. Rev.* **128** 2131
Faddeev L D and Takhtajan L 1981 *Phys. Lett.* A **85** 375
Faddeev L D and Takhtajan L 1984 *Jour. Sov. Math.* **24** 241
[2] Haldane F D M 1983 *Phys. Lett.* A **93** 464
Haldane F D M 1983 *Phys. Rev. Lett.* **50** 1153
[3] Dender D C, Davidovic D, Reich D H, Broholm C, Lefman K and Aeppli G 1996 *Phys. Rev.* B **53** 2583
[4] Dender D C, Hammar P R, Reich D H, Broholm C and Aeppli G 1997 *Phys. Rev. Lett.* **79** 1750
[5] Helfrich R, Köppen M, Lang M, Steglich F and Ochiai A 1998 *J. Magn. Magn. Mater.* **177–181** 309
Köppen M *et al* 1999 *Phys. Rev. Lett.* **82** 4548
[6] Oshikawa M and Affleck I 1997 *Phys. Rev. Lett.* **79** 2883
[7] Affleck I and Oshikawa M 1999 *Phys. Rev.* B **60** 1038

[8] Oshikawa M, Ueda K, Aoki H, Ochiai A and Kohgi M 1999 *J. Phys. Soc. Japan* **68** 3181
[9] Date M, Yamazaki H and Motokawa M 1970 *Suppl. Progr. Theor. Phys.* **46** 194
[10] Ishida T, Nakayama K, Nakagawa M, Sato W, Ishikawa Y, Yasui M, Iwasaki F and Nogami T 1997 *Synth. Metals* **85** 1655
Ishida I and Nogami T 1997 *Recent Res. Devel. in Pure and Applied Chem.* 1
[11] Rodriguez-Carvajal J 1990 *Abstracts of Satellite Meeting on Powder Diffraction of the XV Congress of the IUCr (Toulouse)* p 127
[12] Kelnberger A 1996 *Thesis* Technical University Berlin
[13] Yasui M, Ishikawa Y, Akiyama N, Ishida T, Nogami T and Iwasaki F 2000 *Acta Crystallogr.* B, submitted
[14] Pilawa B 1999 private communication
[15] Yamada I, Nishi M and Akimitsu J 1996 *J. Phys.: Condens. Matter* **8** 2625
[16] Oshikawa M and Affleck I 1999 *Phys. Rev. Lett.* **82** 5136
[17] Feyerherm R, Ishida T, Nogami T and Steiner M 1999 *Mol. Cryst. Liq. Cryst.* **335** 947
[18] Bonner J C and Fisher M E 1964 *Phys. Rev.* **135** A640
[19] Eggert S, Affleck I and Takahashi M 1994 *Phys. Rev. Lett.* **73** 332
[20] Essler F H L 1999 *Phys. Rev.* B **59** 14 376
Oshikawa M 2000 private communication
[21] Affleck I and Oshikawa M 2000 private communication
[22] Feyerherm R 2000 unpublished
[23] Takeda K, Matsukawa S and Haseda T 1971 *J. Phys. Soc. Japan* **30** 1330
[24] Koyama M, Suzuki H and Watanabe T 1976 *J. Phys. Soc. Japan* **40** 1564
[25] Hammar P R, Stone M B, Reich D H, Broholm C, Gibson P J, Turnbull M M, Landee C P and Oshikawa M 1999 *Phys. Rev.* B **59** 1008